Organic & Biomolecular Chemistry

Cite this: *Org. Biomol. Chem.*, 2012, **10**, 7282

www.rsc.org/obc

PAPER

Investigating the effect of macrocycle size in anion templated imidazolium-based interpenetrated and interlocked assemblies†

Graeme T. Spence, Nicholas G. White and Paul D. Beer*

Received 28th June 2012, Accepted 24th July 2012
DOI: 10.1039/c2ob26237a

The effect of varying the size of the macrocycle component on the formation of anion templated imidazolium interpenetrated assemblies is investigated. Two different approaches to reducing the macrocycle size are undertaken and the stabilities of the resulting pseudorotaxanes incorporating substituted imidazolium threading components studied using ^{1}H NMR spectroscopy. Novel imidazolium axle containing interlocked rotaxane host structures are synthesised using chloride anion templated amide condensation and 'stoppering' methods, and the anion recognition properties of the 'stoppered' rotaxane investigated.

Introduction

The positively charged imidazolium heterocycle is capable of effective anion complexation *via* strong electrostatic and hydrogen bonding interactions, and hence has been widely employed in a variety of acyclic and macrocyclic anion receptor and sensing systems.[1–9]

Through careful design, the anion templated synthesis of mechanically interlocked structures can result in the construction of potent and selective anion receptors possessing three dimensional host cavities, with recent systems exploiting a variety of anion binding groups.[10–15]

In a previous investigation,[16] substituted imidazolium threads with contrasting hydrogen bond donor arrangements, 4,5-dimethylimidazolium **1**·Cl and 2-methylimidazolium **2**·Cl (Fig. 1), were demonstrated to form stable chloride anion templated pseudorotaxane assemblies with isophthalamide macrocycle **3** *via* favourable, cooperative amide–halide hydrogen bonding and aromatic donor–acceptor interactions between the electron-rich macrocycle hydroquinone groups and electron-deficient imidazolium motifs. Furthermore, the corresponding imidazolium axle containing rotaxane host systems displayed selectivity for halide guest species over larger, more basic oxoanions.[17]

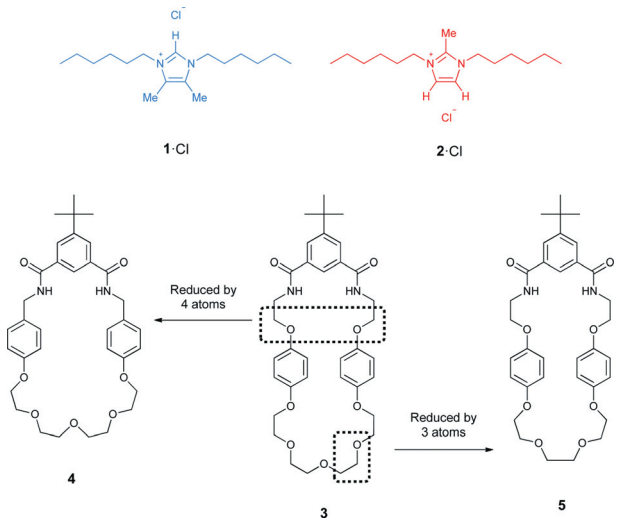

Fig. 1 4,5-Dimethyl- and 2-methylimidazolium threads **1**·Cl and **2**·Cl and macrocycles **3**, **4** and **5**.

In an effort to ultimately further improve the anion recognition properties of such interlocked hosts, we describe herein an investigation into the effect of reducing the size of the macrocycle component on anion templated pseudorotaxane assembly stability and in the construction of novel imidazolium-based rotaxanes.‡

Chemistry Research Laboratory, Department of Chemistry, University of Oxford, Mansfield Road, Oxford OX1 3TA, UK.
E-mail: paul.beer@chem.ox.ac.uk; Fax: +44 (0) 1865 272609;
Tel: +44 (0) 1865 285142

†Electronic supplementary information (ESI) available: Spectral characterisation of novel compounds, 2D ^{1}H-^{1}H ROESY spectra, ^{1}H NMR titration protocols and data, discussion of pseudorotaxane equilibria, and crystallographic information. CCDC 888917 and 888918. For ESI and crystallographic data in CIF or other electronic format see DOI: 10.1039/c2ob26237a

‡With the same objective of optimising the properties of functional interlocked structures through strategic design modifications, the effect of reducing the macrocycle size on a number of other systems has also been reported recently.[29,30]

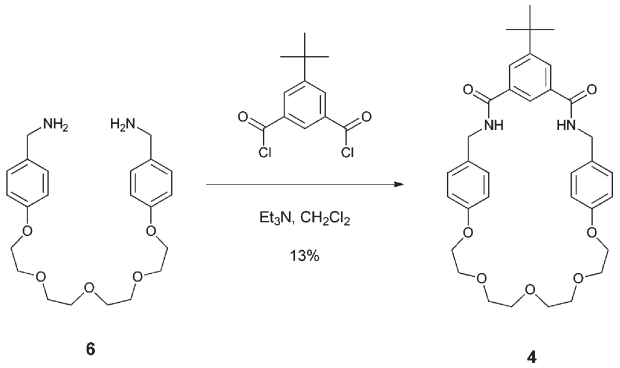

Scheme 1 Synthesis of macrocycle **4**.

Results and discussion

Macrocycle synthesis

Two different design strategies for reducing the size of macrocycle **3** were undertaken, as shown in Fig. 1. Firstly, in the case of macrocycle **4**, the linker between the isophthalamide binding cleft and the electron-rich aromatic groups, in this case phenolic rather than hydroquinone, was shortened, reducing the macrocycle size by four atoms. Secondly, for macrocycle **5**,[18] three atoms were removed from the polyether chain of **3**.

Whilst similar macrocycle derivatives to **4** have been reported,[19–21] this system is novel due to the *tert*-butyl functionalisation of the isophthalamide motif, which is necessary for direct comparison with macrocycles **3** and **5**. Condensation of bis-amine **6**[20] with 5-(*tert*-butyl)isophthaloyl dichloride in the presence of 2.5 equivalents of Et_3N gave macrocycle **4** in 13% yield (Scheme 1).§

Crystals of macrocycle **4** suitable for single-crystal X-ray diffraction structural analysis were obtained by recrystallisation from MeCN and analysed using synchrotron radiation at Diamond Light Source beamline I19 (Fig. 2). In the solid-state, the amide groups of **4** are approximately *syn–anti* and form an extended hydrogen bonding network with the amide and polyether groups of adjacent macrocycles.

Pseudorotaxane investigations

Initially, ^{1}H NMR pseudorotaxane assembly studies were carried out in $CDCl_3$ using macrocycle **4** and imidazolium threading components **1**·Cl and **2**·Cl. The spectra for macrocycle **4**, 4,5-dimethylimidazolium thread **1**·Cl and an equimolar solution of both components are shown in Fig. 3, with the observed chemical shift changes indicative of the formation of anion templated pseudorotaxane **1**·**4**·Cl. Specifically, polarisation of the templating chloride anion away from the thread and towards the macrocycle hydrogen bond donors is responsible for downfield shifts in the signals corresponding to macrocycle protons c and d, and an upfield shift in imidazolium thread proton 1. Additionally, macrocycle phenolic protons g are shifted significantly upfield

§ Significantly higher macrocyclisation yields for similar systems have been achieved using high dilution methods, however these conditions were not used to allow for direct comparison with the yield from the templated reaction discussed later.

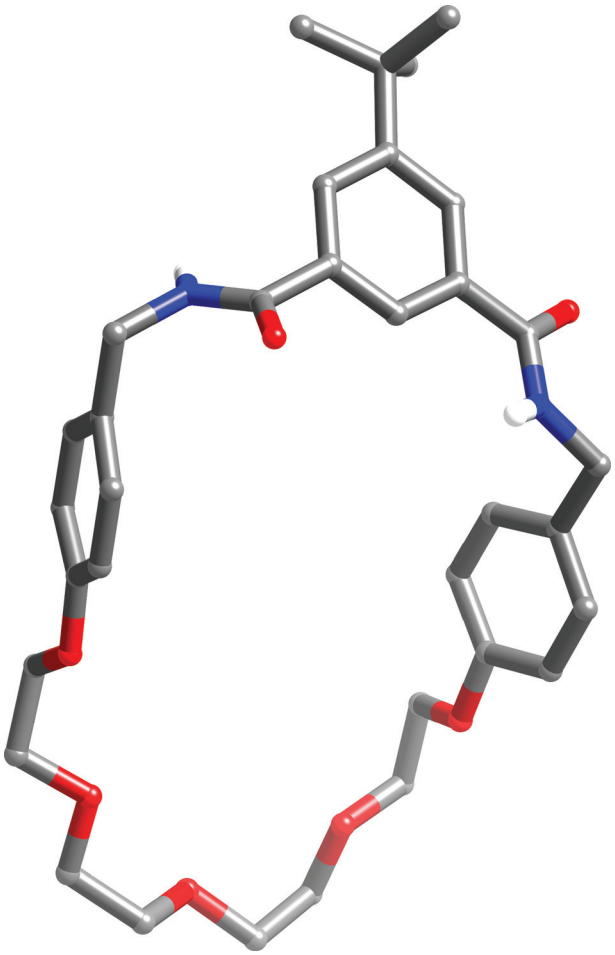

Fig. 2 Crystal structure of macrocycle **4**. Protons and lower occupancy positions of disorder are omitted for clarity.

upon pseudorotaxane formation, due to favourable donor–acceptor interactions with the electron-deficient imidazolium thread. Similar shifts were also observed for the formation of the analogous 2-methylimidazolium pseudorotaxane **2**·**4**·Cl (Fig. 4).

Quantitative ^{1}H NMR titration experiments were then undertaken, with aliquots of threading components **1**·Cl and **2**·Cl added to $CDCl_3$ solutions of macrocycle **4**. In addition, control titrations were carried out using hexafluorophosphate threads **1**·PF_6 and **2**·PF_6, and tetrabutylammonium (TBA) chloride. The macrocycle phenolic protons f and g were monitored throughout all of the titration experiments and the shifts observed are shown in Fig. S11 (ESI†). The minor shifts in the signal corresponding to protons g during the control titrations ($\Delta\delta \leq 0.07$ ppm) indicate that the significant upfield shifts observed upon addition of **1**·Cl and **2**·Cl ($\Delta\delta$ = −0.44 and −0.43 ppm respectively) are not simply due to the macrocycle sequestering the anion, and that pseudorotaxane formation requires the presence of the halide template. Further evidence for pseudorotaxane formation was obtained from 2D ^{1}H-^{1}H NMR ROESY spectroscopy, with several intercomponent correlations observed for both systems, as shown in Fig. S7 and S8.†

Moreover, crystals of **2**·**4**·Cl suitable for single-crystal X-ray diffraction structural analysis were obtained by slow diffusion of $^iPr_2O$ into an equimolar $CDCl_3$ solution of thread **2**·Cl and

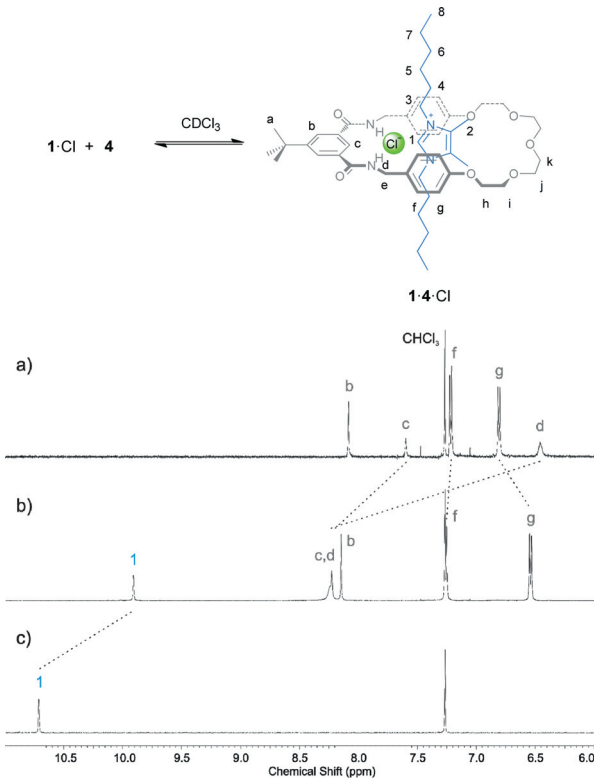

Fig. 3 Partial ^{1}H NMR spectra (500 MHz) in $CDCl_3$ at 293 K of (a) macrocycle **4**, (b) macrocycle **4** plus 1.0 equivalent of thread **1**·Cl, and (c) thread **1**·Cl.

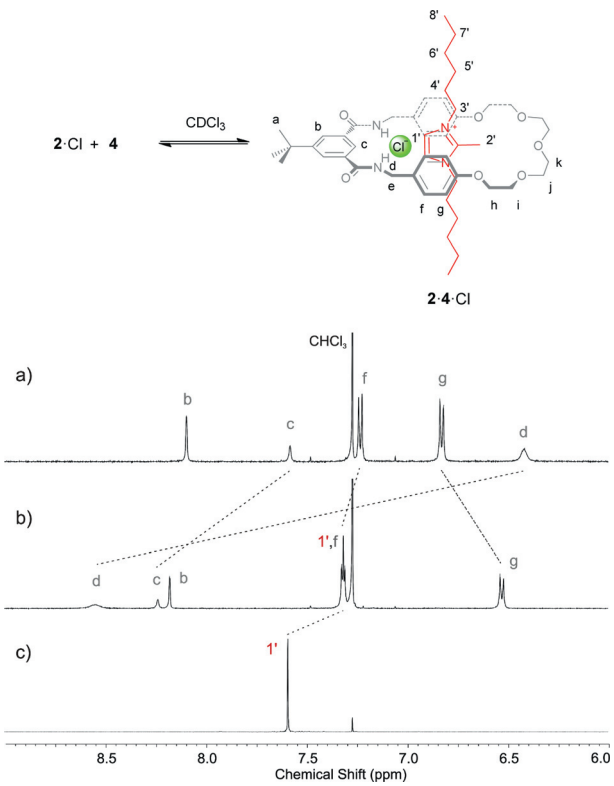

Fig. 4 Partial ^{1}H NMR spectra (500 MHz) in $CDCl_3$ at 293 K of (a) macrocycle **4**, (b) macrocycle **4** plus 1.0 equivalent of thread **2**·Cl, and (c) thread **2**·Cl.

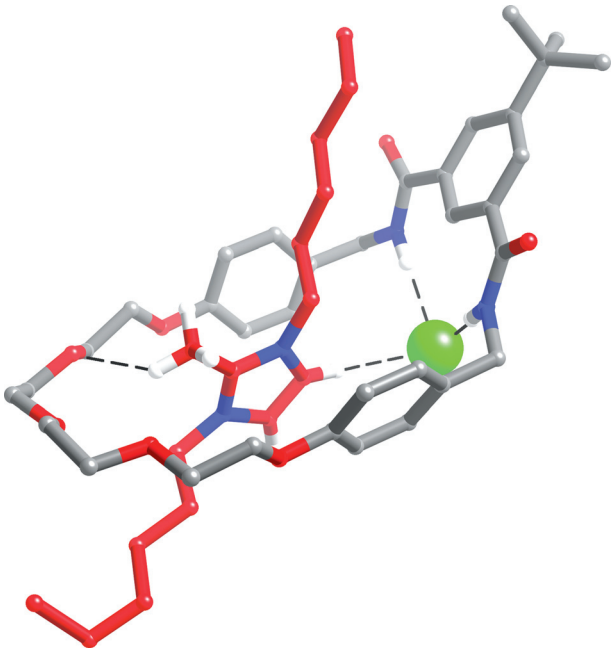

Fig. 5 Crystal structure of pseudorotaxane **2**·**4**·Cl. One of the two independent pseudorotaxane assemblies in the asymmetric unit is shown. H···Cl and H···O close contacts are displayed using dashed black lines. Protons omitted for clarity where appropriate.

macrocycle **4**. These were found to contain two independent pseudorotaxane assemblies in the asymmetric unit, however each have very similar geometries (with only slight differences in atomic distances) and only one is shown in Fig. 5. In contrast to the analogous pseudorotaxane containing macrocycle **3**,[17] in which strong inter-assembly electrostatic interactions resulted in the imidazolium thread existing in two contrasting orientations within the macrocycle, only one co-conformation is observed for **2**·**4**·Cl, in agreement with the solution phase orientation of the 2-methylimidazolium thread (depicted in Fig. 4). The halide template forms three hydrogen bonds to one of the imidazolium C–H protons (3.467(8) or 3.465(9) Å for the two assemblies in the asymmetric unit) and to the two macrocycle N–H donor atoms (3.254(7)–3.370(11) Å). Hydrogen bonds between the imidazolium methyl protons of the thread and several polyether oxygen atoms of the macrocycle are also observed, with one such close contact shown in Fig. 5 (C···O distance of 3.228(14) or 3.175(15) Å).

To calculate the relative stabilities of assemblies **1**·**4**·Cl and **2**·**4**·Cl, macrocycle amide protons d were monitored throughout the titration experiments (Fig. S12†), and WinEQNMR2[22] analysis determined the pseudorotaxane association constants shown in Table 1. The amide protons were chosen for consistency with the previously reported pseudorotaxane studies using macrocycle **3**, the results of which are also shown in Table 1.[16] It should be noted that these values are apparent 1 : 1 association constants for ternary complexes. However, as discussed in the ESI,† the other equilibria present are insignificant compared with the intended association, indicating that these values do indeed reflect the relative stabilities of the anion templated pseudorotaxane assemblies.

In addition, analogous titration experiments were undertaken using macrocycle **5**, with the observed shifts in agreement with those seen in previous pseudorotaxane investigations.[16,18] Again,

Table 1 Association constants, K_{app} (M^{-1}), for pseudorotaxane formation using macrocycles **3**, **4** and **5** and threading components **1**·Cl and **2**·Cl in $CDCl_3$ at 293 K. Obtained by monitoring macrocycle amide protons d. Errors are given in parentheses

Guest	Macrocycle **3**[16]	Macrocycle **4**	Macrocycle **5**
1·Cl	97 (3)	644 (24)	101 (6)
2·Cl	245 (5)	3287 (177)	258 (9)

the amide protons were monitored throughout these experiments (Fig. S14†) to give the association constants shown in Table 1.

Importantly, for macrocycle **4**, both the 4,5-dimethyl- and 2-methylimidazolium assemblies, **1**·**4**·Cl and **2**·**4**·Cl, exhibit much greater stability when compared with the analogous pseudorotaxane assemblies containing macrocycle **3**, which suggests a higher degree of complementarity exists in these interpenetrated structures. Furthermore, the difference between the systems containing contrasting imidazolium motifs, with the 2-methyl- being significantly more stable than the 4,5-dimethyl-imdazolium, is much more pronounced with macrocycle **4** than **3**.

In contrast, there is no significant difference between the association constants obtained from the titrations with macrocycle **5** compared with the previous studies with macrocycle **3**. Hence, shortening the polyether chain by three atoms, and the associated effect on the hydrogen bonding and donor–acceptor interactions as well as entropic considerations, has had no effect on the overall stabilities of the respective anion templated imidazolium pseudorotaxane assemblies.

To explain these findings, the shifts observed for imidazolium methyl protons (2 and 2′, labelled in Fig. 3 and 4) during the pseudorotaxane titrations were studied (Fig. S13 and S15†). Whilst the methyl protons 2 of **1**·Cl shifted only slightly upon addition to macrocycle **4** ($\Delta\delta$ = +0.08 ppm after 10.0 equivalents, Fig. S13a†), the methyl protons 2′ of **2**·Cl shifted significantly downfield during the corresponding titration ($\Delta\delta$ = +0.70 ppm, Fig. S13b†). These shifts are due to hydrogen bonding between the thread methyl groups and the polyether chain of macrocycle **4**, with the 2-methylimidazolium group of thread **2**·Cl much more favourably aligned for these interactions than the 4,5-dimethylimidazolium groups of **1**·Cl (as depicted in

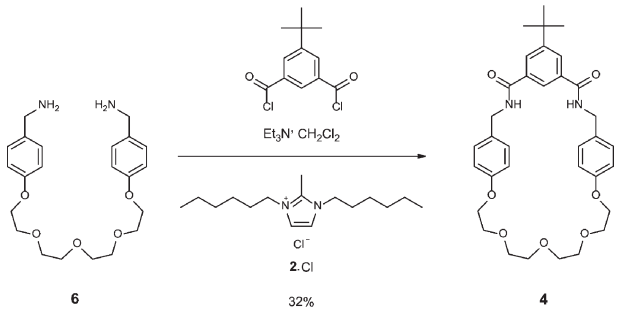

Scheme 2 Templated synthesis of macrocycle **4**.

Fig. 3 and 4). This results in considerable secondary stabilisation of **2**·**4**·Cl, explaining its increased stability compared to **1**·**4**·Cl.

Smaller downfield shifts were observed for these protons in the pseudorotaxane systems containing the other macrocycles, **1**·**3**·Cl and **2**·**3**·Cl ($\Delta\delta$ = −0.01 and +0.08 ppm respectively),[16] and **1**·**5**·Cl, and **2**·**5**·Cl ($\Delta\delta$ = +0.03 and +0.15 ppm respectively, Fig. S15†). These shifts suggest that the observed trend in the pseudorotaxane stabilities of these systems, 2-methylimidazolium greater than 4,5-dimethylimidazolium, is also due to the presence of these hydrogen bonding interactions in the 2-methylimidazolium system. However, the much larger shifts observed for assemblies **1**·**4**·Cl and **2**·**4**·Cl reflect the higher degree of complementarity between the imidazolium threading components and macrocycle **4**. The hydrogen bonding interactions between the imidazolium methyl groups and macrocycle polyether chain do not contribute as much in the 4,5-dimethylimidazolium systems, but the stabilisation from the donor–acceptor interactions is also expected to be increased due to the shortened linker between the anion binding cleft and the electron-rich aromatic groups.

Having demonstrated that reducing the macrocycle size in this specific manner considerably favours chloride anion templated imidazolium pseudorotaxane formation, attempts to synthesise analogous rotaxane structures for anion recognition studies were undertaken. As enhanced hydrogen bonding between the imidazolium methyl group of **2**·Cl and the polyether chain of **4** contributed to the increased pseudorotaxane stabilities, it was decided to synthesise interlocked systems incorporating

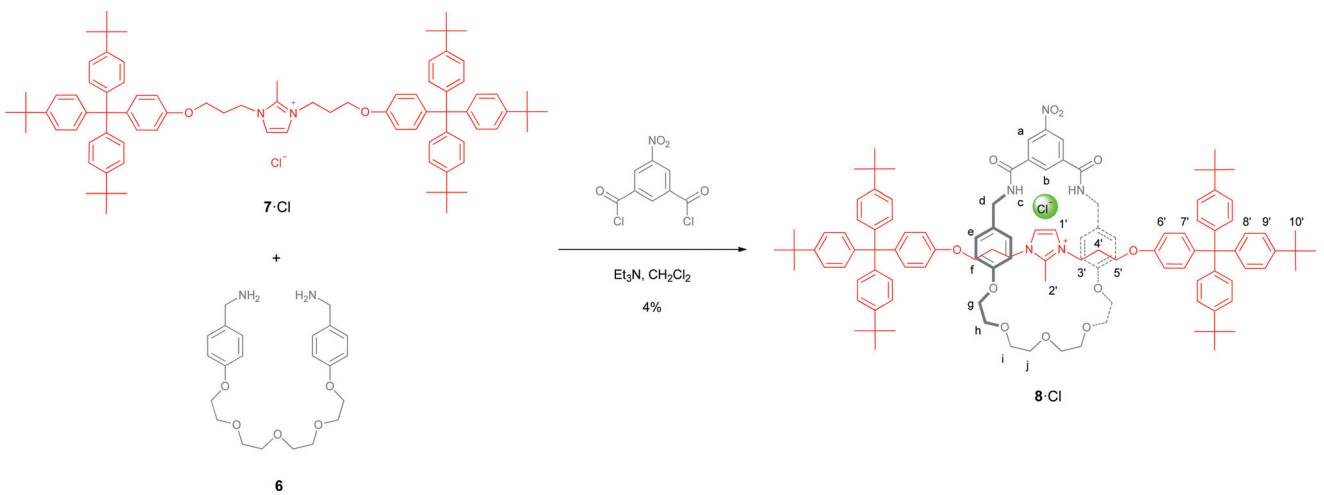

Scheme 3 Synthesis of 2-methylimidazolium rotaxane **8**·Cl *via* a condensation method.

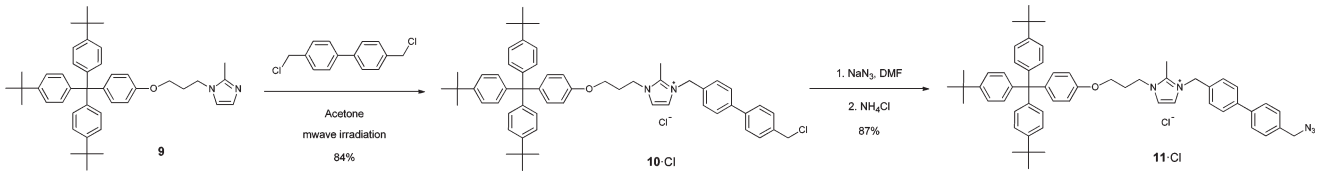

Scheme 4 Synthesis of mono-stoppered 2-methylimidazolium thread **11**·Cl.

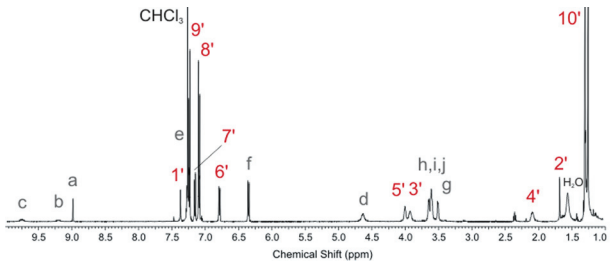

Fig. 6 ^{1}H NMR spectrum (500 MHz) of rotaxane **8**·Cl in $CDCl_3$ at 293 K.

2-methylimidazolium axle components and retaining the five oxygen polyether chain within the macrocycle.

Rotaxane synthesis by condensation

The synthesis of anion templated interlocked structures *via* a novel amide condensation route has recently been established by Beer *et al.* and applied to a number of pyridinium-based systems.[13,23–25] Encouraged by the strong stability of pseudorotaxane assembly **2**·**4**·Cl, the macrocyclisation reaction to form **4** was carried out in the presence of one equivalent of 2-methylimidazolium thread **2**·Cl (Scheme 2). Importantly, a significant enhancement of the yield from 13% to 32% was observed, thus the presence of **2**·Cl in the reaction mixture appears to favour [1 + 1]-macrocyclisation over higher order macrocyclic and oligomeric by-products.

In light of this result, the analogous rotaxane synthesis was attempted using axle **7**·Cl, bis-amine **6** and 5-nitroisophthaloyl dichloride (Scheme 3). Rotaxane **8**·Cl was isolated from the reaction mixture by preparative silica gel thin layer chromatography, but in a very low yield of 4%. The ^{1}H NMR spectrum for 2-methylimidazolium rotaxane **8**·Cl is shown in Fig. 6, with the signal corresponding to macrocycle phenolic protons f appearing further downfield than those in macrocycle **4** (at 6.36 ppm compared with 6.69 ppm). This is in agreement with the analogous shifts observed in the pseudorotaxane investigations (Fig. 4), indicating interlocked structure formation. Additionally, imidazolium methyl protons 2′ are considerably shifted upfield compared to axle **7**·Cl ($\Delta\delta = -1.08$ ppm), presumably due to the macrocycle phenolic ring currents. Further characterisation of the rotaxane was provided by high resolution electrospray mass spectrometry and 2D ^{1}H–^{1}H NMR ROESY spectroscopy, with the interlocked nature of **8**·Cl confirmed by a number of intercomponent ROESY correlations (Fig. S9†).

The synthesis of **8**·Cl was repeated with ten equivalents of bis-amine **6** and 5-nitroisophthaloyl dichloride in an attempt to favour interlocked structure formation, however after removal of the increased oligomeric by-products, ^{1}H NMR integration of the crude mixture revealed no significant enhancement in the rotaxane yield.

Although 2-methylimidazolium rotaxane **8**·Cl is the first non-pyridinium interlocked structure prepared *via* this anion templated condensation strategy, this is not a viable route for the effective synthesis of anion host systems due to the very low yield. It is unclear why this is the case, given that the macrocyclisation yield was considerably enhanced in the presence of thread **2**·Cl.

Rotaxane synthesis by 'stoppering'

To exploit the ability of the 2-methylimidazolium motif to form strong anion templated pseudorotaxanes with macrocycle **4** for effective rotaxane synthesis, an alternative 'threading-followed-by-stoppering' approach was employed. Mono-stoppered 2-methylimidazolium thread **11**·Cl, incorporating a terminal azide group, was synthesised as shown in Scheme 4. Imidazole derivative **9**[17] was reacted with an excess of 4,4′-bis(chloromethyl)-1,1′-biphenyl under microwave irradiation to give the desired alkylated product **10**·Cl in 84% yield. Conversion of the terminal chloro-functionality to the key azide group was achieved using NaN_3, and repeated washing with aqueous NH_4Cl afforded target thread **11**·Cl.

For rotaxane formation *via* 'stoppering', a copper(I)-catalysed alkyne-azide cycloaddition (CuAAC) reaction between azide

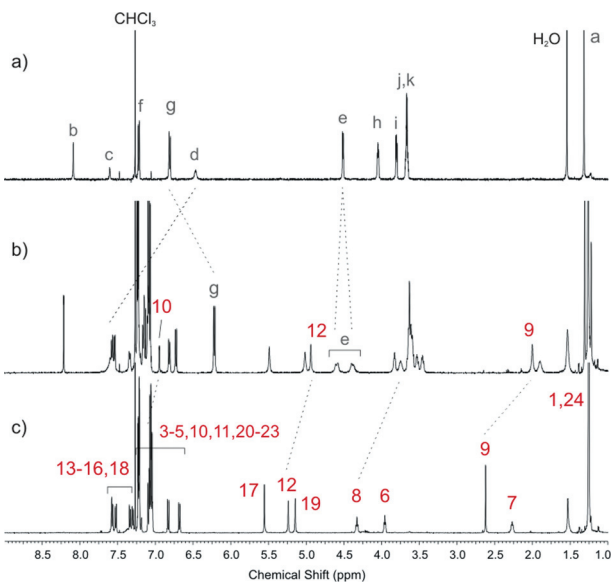

Fig. 7 ^{1}H NMR spectra (500 MHz) in $CDCl_3$ at 293 K of (a) macrocycle **4**, (b) rotaxane **13**·PF_6, and (c) axle **14**·PF_6.

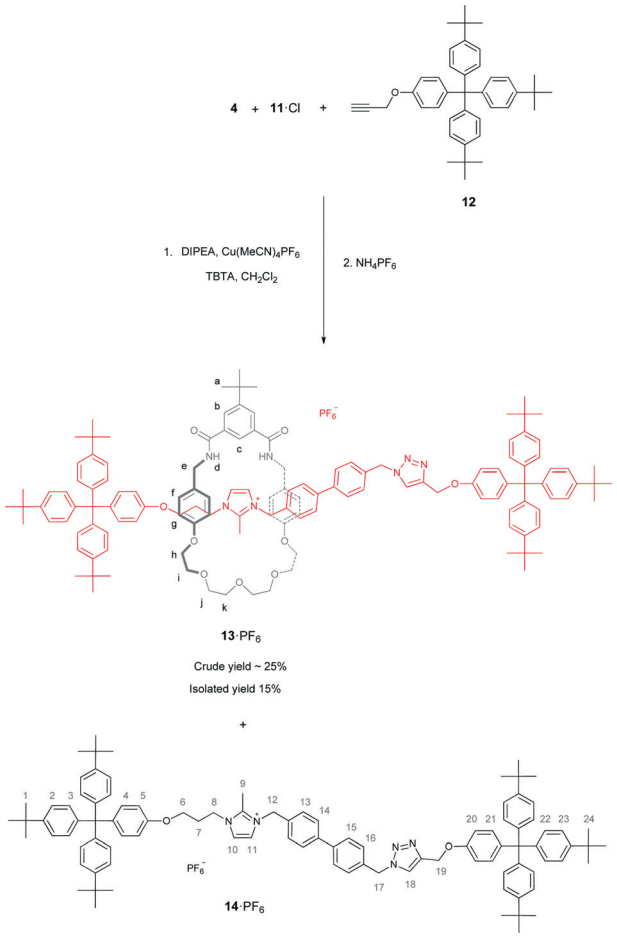

Scheme 5 Synthesis of 2-methylimidazolium rotaxane **13**·PF_6 *via* a 'stoppering' method.

11·Cl and stoppered alkyne **12**[26] was undertaken in the presence of macrocycle **4** (one equivalent compared to **11**·Cl), using DIPEA as the base, $Cu(MeCN)_4PF_6$ as the catalyst and TBTA as a stabilising ligand (Scheme 5). Although ^{1}H NMR integration of the reaction mixture indicated a crude yield of approximately 25% for interlocked structure formation, difficulties in purification resulted in target rotaxane **13**·PF_6 being isolated in 15% yield following preparative silica gel thin layer chromatography, anion exchange to the hexafluorophosphate salt and trituration with methanol. 'Stoppered' axle **14**·PF_6 was also isolated from the reaction mixture.

To aid purification, rotaxane synthesis was attempted in the absence of the TBTA stabilising ligand. However, in addition to the expected reduction in reaction rate (completion after three days compared to 15 h with TBTA), a considerable loss in the yield of rotaxane was observed (10% by NMR integration). It is not evident why the presence of TBTA would favour interlocked structure formation to such an extent.¶

The ^{1}H NMR spectrum of **13**·PF_6, along with those of its component macrocycle **4** and axle **14**·PF_6, is shown in Fig. 7. Importantly, the signal corresponding to macrocycle phenolic protons g is shifted upfield in rotaxane **13**·PF_6 due to the donor–acceptor interactions characteristic of interlocked structures of this type ($\Delta\delta = -0.47$ ppm). Shielding from the macrocycle electron-rich aromatic groups are responsible for upfield shifts in axle protons 8, 9 and 12, all of which are α- to the imidazolium ring, whilst macrocycle protons e are split in the rotaxane, reflecting the asymmetry of the axle component. Finally, amide protons d appear at a significantly higher chemical shift in interlocked host **13**·PF_6 than in macrocycle **4**.

The interlocked nature of rotaxane **13**·PF_6 was confirmed by high resolution electrospray mass spectrometry and 2D ^{1}H–^{1}H NMR ROESY spectroscopy, and the observed intercomponent ROESY correlations are shown in Fig. S10.† There is the potential for a number of possible interactions between the macrocycle and axle components of rotaxane **13**·PF_6, especially between the macrocycle amide groups and axle triazole unit formed in the 'stoppering' reaction.[27] It was expected that even in the absence of a coordinating anion, the macrocycle would reside primarily over the axle imidazolium group due to the favourable donor–acceptor and methyl–polyether hydrogen bonding interactions, and the observed correlations indicate that this is indeed the case.

Rotaxane anion binding studies

In order to investigate the anion recognition properties of 2-methylimidazolium rotaxane **13**·PF_6, ^{1}H NMR titration experiments were carried out in the competitive 1 : 1 $CDCl_3/CD_3OD$ solvent mixture using a range of TBA anion salts – the halides chloride, bromide and iodide, and oxoanions dihydrogen phosphate and acetate. Spectra from the titration of **13**·PF_6 with TBA chloride are shown in Fig. 8. Throughout the titrations, downfield shifts were observed for the rotaxane cavity protons involved in anion binding *via* C–H hydrogen bonding, namely isophthalamide proton c and amide protons d of the macrocycle and axle imidazolium protons 10 and 11. However, the amide protons (d) were not able to be followed due to deuterium exchange. Interestingly, only moderate shifts in imidazolium protons 10 and 11 were observed, possibly due to opposing contributions from anion binding and donor–acceptor interactions. Importantly, no significant shifts occurred in the signals corresponding to macrocycle phenolic protons g, axle CH_2 protons 9

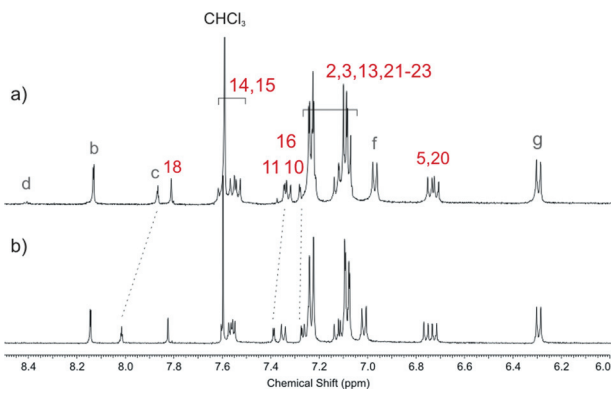

Fig. 8 Partial ^{1}H NMR spectra (500 MHz) in 1 : 1 $CDCl_3/CD_3OD$ at 293 K of (a) rotaxane **13**·PF_6 and (b) rotaxane **13**·PF_6 plus 5.0 equivalents of TBACl.

¶However recent studies have shown that triazole-based stabilising ligands, including TBTA, are able to favour 'click' macrocyclisation over oligomerisation in certain systems.[31,32]

Table 2 Association constants, K (M^{-1}), of rotaxanes **13**·PF_6 and **15**·PF_6 with anions in 1 : 1 $CDCl_3/CD_3OD$ at 293 K. Obtained by monitoring *para*-isophthalamide proton. Errors are given in parentheses

Anion	Rotaxane **13**·PF_6	Rotaxane **15**·PF_6[17]
Cl^-	307 (21)	360 (24)
Br^-	397 (24)	446 (30)
I^-	424 (37)	360 (27)
$H_2PO_4^-$	128 (12)	153 (15)
OAc^-	171 (21)	108 (6)

and 12, and triazole proton 18, indicating no major co-conformational changes occur upon anion binding, and that the axle triazole group does not participate in any interactions with the anion.

Para-isophthalamide proton c was monitored during the titration experiments (Fig. S16†) and 1 : 1 stoichiometric association constants determined using WinEQNMR2 analysis of the data (Table 2).

Rotaxane host **13**·PF_6 exhibits significantly stronger binding for the spherical halide guest species over the larger, more basic oxoanions dihydrogen phosphate and acetate. This selectivity has been achieved by the creation of a three dimensional binding cavity within the interlocked structure, and the behaviour of imidazolium methyl protons 9 during the titrations is evidence for different binding modes for the halides and oxoanions, internal and external to the rotaxane host cavity (Fig. S17†). These protons shift upfield upon addition of the halides ($\Delta\delta = -0.06$ to 0.08 ppm after 10.0 equivalents), slightly downfield with dihydrogen phosphate (+0.03 ppm), and do not shift with acetate (<0.01 ppm). Hence, the contrasting binding modes displayed by **13**·PF_6 appear to alter the position of the imidazolium methyl protons with respect to the hydroquinone ring currents in different ways.

There is little discrimination between the halides, although it does appear that bromide and iodide are bound slightly more strongly than chloride. Furthermore, both the anion binding strength and selectivity are similar to that exhibited by the analogous 2-methylimidazolium rotaxane **15**·PF_6 (Fig. 9 and Table 2), which contains a larger macrocycle component.

It is difficult to make a direct comparison between the anion binding properties of 2-methylimidazolium rotaxanes **13**·PF_6 and **15**·PF_6, due to a number of structural differences arising from their methods of construction, besides a reduction in the size of the macrocycle. Firstly, host **13**·PF_6 contains the 5-*tert*-butyl-isophthalamide motif, compared to the 5-nitro-isophthalamide group of rotaxane **15**·PF_6. The nitro functionalisation increases the acidity of the isophthalamide amide protons, and this has been shown to have a considerable effect on the strength of rotaxane anion binding, for example in one such system a four-fold increase in chloride binding affinity was observed compared with an unsubstituted isophthalamide rotaxane analogue.[28]

Secondly, although the ^1H NMR studies indicate that the macrocycle component of **13**·PF_6 lies predominately over the imidazolium group of the axle, there are several possible co-conformational equilibria arising from the extended asymmetrical axle component. Both of these factors would significantly weaken the anion binding ability of rotaxane **13**·PF_6 compared with **15**·PF_6 and, given that the halide binding strengths of these two systems are approximately equal (~400 M^{-1}), it is

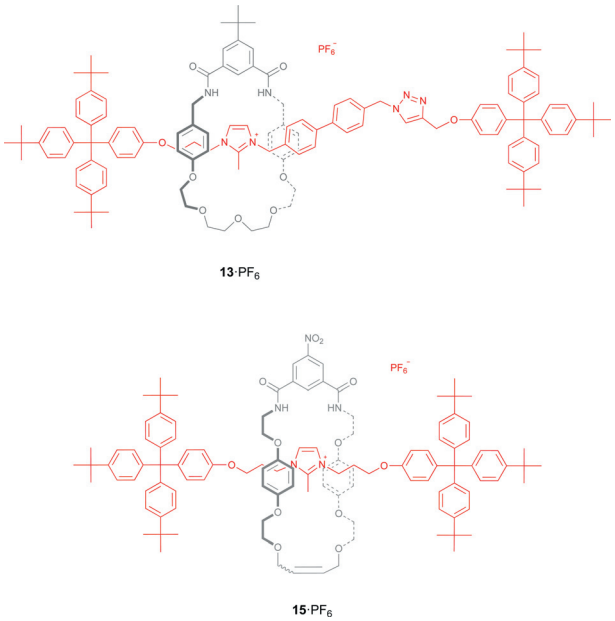

Fig. 9 2-Methylimidazolium rotaxanes **13**·PF_6 and **15**·PF_6.[17]

postulated that reducing the size of the macrocycle component and incorporating the five oxygen polyether chain may be responsible for enhancing anion complexation if these considerations are taken into account.

It is noteworthy that no significant changes in the binding selectivity, either between the halides and oxoanions or within the halides themselves, were observed for **13**·PF_6 in comparison with **15**·PF_6.

Conclusions

The effect of varying the size of the macrocycle on the formation of chloride anion templated imidazolium pseudorotaxane assemblies was investigated using two macrocycle components. Compared with the previously reported systems containing macrocycle **3**, substantial increases in pseudorotaxane stabilities were observed with smaller macrocycle **4**, whilst the use of a different smaller macrocycle, **5**, resulted in no significant differences. The structural arrangement of the isophthalamide, electron-rich aromatic and polyether groups within the macrocycle components is responsible for this difference, as **4** displayed a greater degree of complementarity with the substituted imidazolium threading components due to secondary stabilising hydrogen bonding and donor–acceptor interactions, especially with the 2-methylimidazolium motif. This increase in complementarity was supported by the solid-state pseudorotaxane crystal structure of assembly **2**·**4**·Cl.

A rotaxane structure incorporating a similar macrocycle component and a 2-methylimidazolium axle was synthesised *via* a chloride anion templated amide condensation strategy, however in a very low yield. Successful synthesis of an analogous rotaxane in a reasonable yield was achieved by employing a 'stoppering' method using the CuAAC reaction. This host structure exhibited binding selectivity towards the halides over more basic oxoanions due to the creation of a three dimensional interlocked

cavity. The anion recognition properties of this system are similar to that of a previously reported 2-methylimidazolium rotaxane containing a larger macrocycle component, although a number of factors besides macrocycle size are also thought to affect anion binding.

Experimental

General

Commercially available chemicals were used without further purification unless otherwise stated. Dry solvents were obtained by purging with $N_{2(g)}$ and then passing through an MBraun MPSP-800 column. Water was de-ionised and microfiltered using a Milli-Q Millipore machine. Et_3N was distilled and stored over KOH. All tetrabutylammonium salts, TBTA and $Cu(MeCN)_4PF_6$ were stored in a vacuum desiccator prior to use.

NMR spectra were recorded on Varian Mercury 300, Varian Unity Plus 500 and Bruker AVII 500 (with ^{13}C Cryoprobe) spectrometers at 293 K. Low resolution electrospray ionisation (ESI) mass spectrometry (MS) was performed using a Waters LCT Premier spectrometer, and high resolution ESI MS using a Bruker μTOF spectrometer. Melting points were recorded on a Gallenkamp capillary melting point apparatus and are uncorrected. Microwave reactions were undertaken using a Biotage Initiator 2.0 microwave.

Synthesis

Macrocycle **5**,[18] bis-amine **6**,[20] axle **7**·Cl,[17] imidazole derivative **9**[17] and alkyne **12**[26] were prepared by literature procedures.

Macrocycle 4. *Procedure A*: 5-*tert*-butylisophthalic acid (329 mg, 1.48 mmol) was suspended in $SOCl_2$ (5 mL) and heated at reflux under $N_{2(g)}$ for 15 h. The excess $SOCl_2$ was then removed by distillation, and the residue dried *in vacuo*. The crude dichloride (assumed quantitative conversion) was immediately dissolved in dry CH_2Cl_2 (30 mL) and added dropwise to a solution of bis-amine **6** (600 mg, 1.48 mmol) and Et_3N (0.52 mL, 3.71 mmol) in dry CH_2Cl_2 (75 mL) which had been stirred for 30 min. The reaction mixture was then stirred at room temperature under $N_{2(g)}$ for 2 h, after which time the solution was washed with 10% $HCl_{(aq)}$ (2 × 50 mL) and H_2O (2 × 50 mL) and dried over $MgSO_4$. The solvent was removed *in vacuo* and purified by silica gel column chromatography using 97 : 3 CH_2Cl_2/MeOH followed by 7 : 3 $CHCl_3$/acetone to elute the product as a white solid (117 mg, 0.20 mmol, 13%). *Procedure B*: Same as *A*, but with 2-methylimidazolium thread **2**·Cl (425 mg, 1.48 mmol) added at the same time as bis-amine **6**, yielding the product as described above (280 mg, 0.47 mmol, 32%). Mp > 250 °C. ^1H NMR (300 MHz, $CDCl_3$) δ (ppm) 8.04 (2H, s, H_b), 7.82 (1H, s, H_c), 7.15 (4H, d, ^3J = 8.2 Hz, H_f), 6.69 (4H, d, ^3J = 8.2 Hz, H_g), 6.47 (2H, br s, H_d), 4.51 (4H, d, ^3J = 5.3 Hz, H_e), 3.97–4.02 (4H, m, H_h), 3.77–3.80 (4H, m, H_i), 3.67–3.69 (8H, m, H_j & H_k), 1.30 (9H, s, H_a). ^{13}C NMR (75.5 MHz, $CDCl_3$) δ (ppm) 166.8, 157.9, 152.6, 133.8, 130.3, 129.5, 128.4, 120.7, 114.5, 70.7, 69.6, 67.2, 43.8, 35.0, 31.1 (one peak missing – coincidental). MS-ESI *m/z* 613.2896 ($[M + Na]^+$, $C_{34}H_{42}N_2NaO_7$, calc. 613.2884), 613.3 (100%, $[M + Na]^+$), 1203.7 (15%, $[2M + Na]^+$); 625.3 (50%, $[M + Cl]^-$), 703.3 (100%, $[M + CF_3COO]^-$), 625.3 (30%, $[2M + Cl]^-$).

Rotaxane 8·Cl. 5-Nitroisophthalic acid (14 mg, 0.066 mmol) was suspended in $SOCl_2$ (1 mL) and heated at reflux under $N_{2(g)}$ for 15 h. The excess $SOCl_2$ was then removed by distillation, and the residue dried *in vacuo*. The crude dichloride (assumed quantitative conversion) was immediately dissolved in dry CH_2Cl_2 (5 mL) and added dropwise to a solution of bis-amine **6** (27 mg, 0.066 mmol), axle **7**·Cl (80 mg, 0.066 mmol) and Et_3N (23 μL, 0.166 mmol) in dry CH_2Cl_2 (13 mL) which had been stirred for 30 min. The reaction mixture was then stirred at room temperature under $N_{2(g)}$ for 2 h, after which time the solution was washed with 10% $HCl_{(aq)}$ (2 × 10 mL) and H_2O (2 × 10 mL) and dried over $MgSO_4$. The solvent was removed *in vacuo* and the residue purified by preparative silica gel thin layer chromatography (1 : 1 CH_2Cl_2/MeCN followed by 96 : 4 CH_2Cl_2/MeOH) to yield the product as an off-white solid (5 mg, 0.003 mmol, 4%). Mp 183–185 °C (dec.). ^1H NMR (500 MHz, $CDCl_3$) δ (ppm) 9.78 (2H, br s, H_c), 9.23 (1H, br s, H_b), 9.01 (2H, s, H_a), 7.38 (2H, s, H_1), 7.27–7.30 (4H, m, H_e), 7.23–7.26 (12H, m, H_9), 7.17 (4H, d, ^3J = 8.8 Hz, H_7), 7.09–7.12 (12H, m, H_8), 6.79 (4H, d, ^3J = 8.8 Hz, H_6), 6.36 (4H, d, ^3J = 8.8 Hz, H_f), 4.61–4.65 (4H, m, H_d), 3.98–4.00 (4H, m, H_5), 3.90–3.93 (4H, m, H_3), 3.57–3.65 (12H, m, H_h & H_i & H_j), 3.48–3.51 (4H, m, H_g), 2.04–2.09 (4H, m, H_4), 1.66 (3H, s, H_2), 1.27 (54H, s, H_{10}). ^{13}C NMR (125.8 MHz, $CDCl_3$) δ (ppm) 164.9, 157.1, 156.0, 149.0, 148.4, 144.0, 143.4, 140.1, 136.4, 133.6, 132.4, 130.6, 130.4, 126.2, 124.1, 121.5, 113.1, 112.9, 71.1, 70.5, 67.8, 66.7, 64.3, 63.1, 53.4, 45.8, 42.3, 34.3, 31.4, 8.0 (one peak missing – coincidental). MS-ESI *m/z* 1752.0318 ($[M - Cl]^+$, $C_{114}H_{136}N_5O_{11}$, calc. 1752.0264), 1751.9 ($[M - Cl]^+$) – only observed peak in low resolution mass spectrum.

Thread 10·Cl. Imidazole derivative **9** (300 mg, 0.48 mmol) and 4,4′-bis(chloromethyl)-1,1′-biphenyl (600 mg, 0.68 mmol) were dissolved in acetone (30 mL) and heated under microwave irradiation at 150 °C for 2 h. The solvent was then removed *in vacuo* and the residue purified by silica gel gradient column chromatography using 95 : 5 to 85 : 15 CH_2Cl_2/MeOH to elute the product as a white solid (353 mg, 0.40 mmol, 84%). Mp > 250 °C. ^1H NMR (300 MHz, $CDCl_3$) δ (ppm) 7.62 (1H, d, ^3J = 2.4 Hz, NC–*H*), 7.57 (2H, d, ^3J = 8.0 Hz, Ar–*H*), 7.54 (1H, d, ^3J = 2.4 Hz, NC–*H*), 7.51 (2H, d, ^3J = 8.0 Hz, Ar–*H*), 7.44 (2H, d, ^3J = 8.0 Hz, Ar–*H*), 7.40 (2H, d, ^3J = 8.0 Hz, Ar–*H*), 7.20–7.26 (6H, m, Ar–*H*), 7.03–7.11 (8H, m, Ar–*H*), 6.67 (2H, d, ^3J = 8.8 Hz, OAr–*H*), 5.57 (2H, s, N–CH_2–Ar), 4.63 (2H, s, –CH_2–Cl), 4.51 (2H, t, ^3J = 6.5 Hz, N–CH_2–CH$_2$), 4.02 (2H, t, ^3J = 5.6 Hz, O–CH_2–CH$_2$), 2.84 (3H, s, NC–CH_3), 2.37–2.41 (2H, m, CH$_2$–CH_2–CH$_2$), 1.30 (27H, s, –^{t}Bu). ^{13}C NMR (75.5 MHz, $CDCl_3$) δ (ppm) 155.7, 148.3, 144.1, 143.9, 141.2, 140.4, 139.9, 137.0, 132.4, 132.1, 130.6, 129.1, 128.8, 128.0, 127.3, 124.0, 122.3, 121.8, 112.8, 63.6, 63.0, 52.0, 50.6, 45.8, 34.2, 31.3, 29.2, 10.8 (one peak missing – coincidental). MS-ESI *m/z* 841.4869 ($[M - Cl]^+$, $C_{58}H_{66}ClN_2O$, calc. 841.4858), 841.4 ($[M - Cl]^+$) – only observed peak in low resolution mass spectrum.

Thread 11·Cl. Imidazolium **10**·Cl (350 mg, 0.40 mmol) and NaN_3 (78 mg, 1.20 mmol) were dissolved in DMF (15 mL) and

heated at 80 °C under $N_{2(g)}$ for 15 h. After this time, H_2O (40 mL) was added and the crude product extracted with CH_2Cl_2 (3 × 50 mL). The combined organic fractions were washed with H_2O (1 × 20 mL), dried over $MgSO_4$ and the solvent removed *in vacuo*. The resulting residue was dissolved in CH_2Cl_2 (15 mL), washed with 1.0 M $NH_4Cl_{(aq)}$ (5 × 10 mL), H_2O (2 × 10 mL) and brine (1 × 10 mL), and dried over $MgSO_4$. The solvent was then removed *in vacuo* to yield the product as a white solid (306 mg, 0.35 mmol, 87%). Mp > 250 °C. ^{1}H NMR (300 MHz, $CDCl_3$) δ (ppm) 7.64 (1H, d, ^3J = 2.3 Hz, NC–*H*), 7.51–7.60 (5H, m, 2 × Ar–*H* & NC–*H*), 7.35–7.42 (4H, m, 2 × Ar–*H*), 7.20–7.26 (6H, m, Ar–*H*), 7.03–7.11 (8H, m, Ar–*H*), 6.68 (2H, d, ^3J = 8.8 Hz, OAr–*H*), 5.58 (2H, s, N–C*H*$_2$–Ar), 4.51 (2H, t, ^3J = 6.8 Hz, N–C*H*$_2$–CH$_2$), 4.39 (2H, s, –C*H*$_2$–N$_3$), 4.02 (2H, t, ^3J = 5.6 Hz, O–C*H*$_2$–CH$_2$), 2.84 (3H, s, NC–C*H*$_3$), 2.37–2.42 (2H, m, CH$_2$–C*H*$_2$–CH$_2$), 1.30 (27H, s, –^{t}Bu). ^{13}C NMR (75.5 MHz, $CDCl_3$) δ (ppm) 155.7, 148.4, 144.1, 144.0, 141.3, 140.4, 139.8, 134.9, 132.4, 132.0, 130.6, 128.8, 128.7, 128.0, 127.5, 124.1, 122.3, 121.8, 112.8, 63.5, 63.0, 54.4, 52.1, 45.9, 34.3, 31.3, 29.2, 10.8 (one peak missing – coincidental). MS-ESI *m*/*z* 848.5257 ([M − Cl]$^+$, $C_{58}H_{66}N_5O$, calc. 848.5262), 848.5 ([M − Cl]$^+$) – only observed peak in low resolution mass spectrum.

Rotaxane 13·PF$_6$. To a solution of macrocycle **4** (67 mg, 0.113 mmol), azide **11**·Cl (100 mg, 0.113 mmol) and alkyne **12** (74 mg, 0.136 mmol) in dry CH_2Cl_2 (25 mL) was added TBTA (6 mg, 0.011 mmol) and DIPEA (39 µl, 0.226 mmol) followed by $Cu(MeCN)_4PF_6$ (8 mg, 0.023 mmol). The reaction mixture was stirred under $N_{2(g)}$ for 72 h and then the solvent removed *in vacuo*. Purification was undertaken by preparative silica gel thin layer chromatography using 94 : 6 CH_2Cl_2/MeOH. The crude product was dissolved in CH_2Cl_2 (10 mL), washed with 0.1 M $NH_4PF_{6(aq)}$ (10 × 5 mL) and H_2O (4 × 5 mL), and dried over $MgSO_4$. The solvent was removed was then removed *in vacuo* and the residue triturated with methanol (3 × 3 mL) to yield the product as an off-white solid (36 mg, 0.017 mmol, 15%). ^{1}H NMR (500 MHz, $CDCl_3$) δ (ppm) 8.22 (2H, d, ^3J = 1.5 Hz, H$_b$), 7.53–7.63 (7H, m, H$_c$ & H$_d$ & H$_{14}$ & H$_{15}$), 7.34 (2H, d, ^3J = 7.8 Hz, H$_{16}$), 7.20–7.26 (15H, m, H$_2$ & H$_{13}$ & H$_{18}$ & H$_{23}$), 7.13–7.18 (6H, m, H$_f$ & H$_4$), 7.06–7.11 (15H, m, H$_3$ & H$_{11}$ & H$_{21}$ & H$_{22}$), 6.95 (1H, d, ^3J = 2.0 Hz, H$_{10}$), 6.82 (2H, d, ^3J = 8.8 Hz, H$_{20}$), 6.73 (2H, d, ^3J = 8.8 Hz, H$_5$), 6.22 (4H, d, ^3J = 8.3 Hz, H$_g$), 5.49 (2H, s, H$_{17}$), 5.02 (2H, s, H$_{19}$), 4.94 (2H, s, H$_{12}$), 4.60 (2H, d, ^2J = 13.2 Hz, H$_{e'}$), 4.38 (2H, d, ^2J = 13.2 Hz, H$_{e''}$), 3.81–3.85 (2H, m, H$_6$), 3.72–3.77 (2H, m, H$_8$), 3.57–3.67 (12H, m, H$_i$ & H$_j$ & H$_k$), 3.50–3.55 (2H, m, H$_{h'}$), 3.44–3.48 (2H, m, H$_{h''}$), 1.99–2.02 (3H, m, H$_9$), 1.87–1.92 (2H, m, H$_7$), 1.31 (9H, s, H$_a$), 1.26 (27H, s, H$_1$ or H$_{24}$), 1.26 (27H, s, H$_1$ or H$_{24}$). ^{19}F NMR (282.5 MHz, $CDCl_3$) δ (ppm) − 71.8 (d, ^1J = 714 Hz, P*F*$_6$). ^{13}C NMR (125.8 MHz, $CDCl_3$) δ (ppm) 167.6, 156.8, 156.1, 156.0, 152.2, 148.4, 148.3, 144.0, 142.9, 141.4, 140.5, 140.4, 140.2, 134.2, 134.1, 133.9, 132.4, 132.3, 131.7, 130.7, 130.6, 130.3, 129.9, 128.8, 128.5, 128.0, 127.9, 124.1, 124.0, 122.7, 122.1, 120.5, 113.2, 113.1, 112.9, 71.2, 70.7, 70.0, 66.8, 64.1, 63.1, 62.0, 53.9, 51.4, 45.4, 42.0, 35.0, 34.3, 31.4, 31.2, 29.7, 29.1, 8.9 (five peaks missing – coincidental). MS-ESI *m*/*z* 1002.5831 ([M − PF$_6$ + Na]$^{2+}$, $C_{132}H_{154}N_7NaO_9$, calc. 1002.5864), 1002.6 (85%, [M − PF$_6$ + Na]$^{2+}$), 1981.9 (100%, [M − PF$_6$]$^+$).

Axle 14·PF$_6$. Isolated from the reaction mixture for the preparation of rotaxane **13**·PF$_6$ as a white solid. ^{1}H NMR (500 MHz, $CDCl_3$) δ (ppm) 7.56–7.59 (3H, m, H$_{14}$ & H$_{18}$), 7.53 (2H, d, ^3J = 8.1 Hz, H$_{15}$), 7.34 (2H, d, ^3J = 8.1 Hz, H$_{16}$), 7.30 (2H, d, ^3J = 8.1 Hz, H$_{13}$), 7.21–7.24 (13H, m, H$_2$ & H$_{11}$ & H$_{23}$), 7.19 (1H, s, H$_{10}$), 7.03–7.11 (16H, m, H$_3$ & H$_4$ & H$_{21}$ & H$_{22}$), 6.83 (2H, d, ^3J = 8.8 Hz, H$_{20}$), 6.68 (2H, d, ^3J = 9.3 Hz, H$_5$), 5.56 (2H, s, H$_{17}$), 5.24 (2H, s, H$_{12}$), 5.15 (2H, s, H$_{19}$), 4.33 (2H, t, ^3J = 6.6 Hz, H$_8$), 3.96 (2H, t, ^3J = 5.4 Hz, H$_6$), 2.62 (3H, s, H$_9$), 2.24–2.29 (2H, m, H$_7$), 1.26 (27H, s, H$_1$ or H$_{24}$), 1.25 (27H, s, H$_1$ or H$_{24}$). ^{19}F NMR (282.5 MHz, $CDCl_3$) δ (ppm) − 73.3 (d, ^1J = 713 Hz, P*F*$_6$). ^{13}C NMR (75.5 MHz, $CDCl_3$) δ (ppm) 156.1, 155.7, 148.4, 148.3, 144.8, 144.2, 144.0, 143.9, 141.1, 140.4, 140.4, 140.2, 134.0, 132.4, 132.3, 132.0, 130.7, 130.6, 128.8, 128.7, 128.1, 127.8, 124.1, 124.0, 122.6, 122.1, 121.7, 113.1, 112.8, 63.5, 63.0, 62.0, 53.8, 52.1, 45.9, 34.3, 31.4, 29.2, 10.9 (three peaks missing – coincidental). MS-ESI *m*/*z* 1391.8887 ([M − PF$_6$]$^+$, $C_{98}H_{112}N_5O_2$, calc. 1391.8843), 1391.8 (100%, [M − PF$_6$]$^+$) – only observed peak in low resolution mass spectrum.

Acknowledgements

G.T.S. thanks the EPSRC for a studentship (EP/F011504). N.G.W. thanks the Clarendon Fund and Trinity College for a studentship, and the Oxford University Crystallography Service for instrument use. We are grateful to Diamond Light Source for an award of beamtime on Beamline I19.

Notes and references

1 E. Alcalde, N. Mesquida, L. Perez-Garcia, C. Alvarez-Rua, S. Garcia-Granda and E. Garcia-Rodriguez, *Chem. Commun.*, 1999, 295–296.
2 K. Sato, S. Arai and T. Yamagishi, *Tetrahedron Lett.*, 1999, **40**, 5219–5222.
3 J. Yoon, S. K. Kim, N. J. Singh and K. S. Kim, *Chem. Soc. Rev.*, 2006, **35**, 355–360.
4 D. Wang, X. Zhang, C. He and C. Duan, *Org. Biomol. Chem.*, 2010, **8**, 2923–2925.
5 Z. Xu, S. K. Kim and J. Yoon, *Chem. Soc. Rev.*, 2010, **39**, 1457–1466.
6 C. J. Serpell, J. Cookson, A. L. Thompson and P. D. Beer, *Chem. Sci.*, 2011, **2**, 494–500.
7 Z. Xu, N. J. Singh, S. K. Kim, D. R. Spring, K. S. Kim and J. Yoon, *Chem.–Eur. J.*, 2011, **17**, 1163–1170.
8 N. Ahmed, B. Shirinfar, I. S. Youn, A. Bist, V. Suresh and K. S. Kim, *Chem. Commun.*, 2012, **48**, 2662–2664.
9 H.-Y. Gong, B. M. Rambo, V. M. Lynch, K. M. Keller and J. L. Sessler, *Chem.–Eur. J.*, 2012, **18**, 7803–7809.
10 A. Caballero, F. Zapata, N. G. White, P. J. Costa, V. Félix and P. D. Beer, *Angew. Chem., Int. Ed.*, 2012, **51**, 1876–1880.
11 Y. Zhao, Y. Li, Y. Li, H. Zheng, X. Yin and H. Liu, *Chem. Commun.*, 2010, **46**, 5698–5700.
12 N. L. Kilah, M. D. Wise, C. J. Serpell, A. L. Thompson, N. G. White, K. E. Christensen and P. D. Beer, *J. Am. Chem. Soc.*, 2010, **132**, 11893–11895.
13 L. M. Hancock, L. C. Gilday, S. Carvalho, P. J. Costa, V. Félix, C. J. Serpell, N. L. Kilah and P. D. Beer, *Chem.–Eur. J.*, 2010, **16**, 13082–13094.
14 M. K. Chae, J.-M. Suk and K.-S. Jeong, *Tetrahedron Lett.*, 2010, **51**, 4240–4242.

15 M. D. Lankshear and P. D. Beer, *Acc. Chem. Res.*, 2007, **40**, 657–668.
16 C. J. Serpell, N. L. Kilah, P. J. Costa, V. Félix and P. D. Beer, *Angew. Chem., Int. Ed.*, 2010, **49**, 5322–5326.
17 G. T. Spence, C. J. Serpell, J. Sardinha, P. J. Costa, V. Félix and P. D. Beer, *Chem.–Eur. J.*, 2011, **17**, 12955–12966.
18 M. R. Sambrook, P. D. Beer, J. A. Wisner, R. L. Paul, A. R. Cowley, F. Szemes and M. G. B. Drew, *J. Am. Chem. Soc.*, 2005, **127**, 2292–2302.
19 D. A. Leigh and A. R. Thomson, *Org. Lett.*, 2006, **8**, 5377–5379.
20 M. J. Barrell, D. A. Leigh, P. J. Lusby and A. M. Z. Slawin, *Angew. Chem., Int. Ed.*, 2008, **47**, 8036–8039.
21 M. Chen, S. Han, L. Jiang, S. Zhou, F. Jiang, Z. Xu, J. Liang and S. Zhang, *Chem. Commun.*, 2010, **46**, 3932–3934.
22 M. J. Hynes, *J. Chem. Soc., Dalton Trans.*, 1993, 311–312.
23 N. H. Evans, C. J. Serpell and P. D. Beer, *Chem. Commun.*, 2011, **47**, 8775–8777.
24 L. M. Hancock, L. C. Gilday, N. L. Kilah, C. J. Serpell and P. D. Beer, *Chem. Commun.*, 2011, **47**, 1725–1727.
25 N. H. Evans, C. J. Serpell and P. D. Beer, *New J. Chem.*, 2011, **35**, 2047–2053.
26 V. Aucagne, K. D. Hänni, D. A. Leigh, P. J. Lusby and D. B. Walker, *J. Am. Chem. Soc.*, 2006, **128**, 2186–2187.
27 H. Zheng, W. Zhou, J. Lv, X. Yin, Y. Li, H. Liu and Y. Li, *Chem.–Eur. J.*, 2009, **15**, 13253–13262.
28 M. R. Sambrook, P. D. Beer, M. D. Lankshear, R. F. Ludlow and J. A. Wisner, *Org. Biomol. Chem.*, 2006, **4**, 1529–1538.
29 H. Lahlali, K. Jobe, M. Watkinson and S. M. Goldup, *Angew. Chem., Int. Ed.*, 2011, **50**, 4151–4155.
30 K. Hirose, K. Ishibashi, Y. Shiba, Y. Doi and Y. Tobe, *Chem.–Eur. J.*, 2008, **14**, 5803–5811.
31 G. Chouhan and K. James, *Org. Lett.*, 2011, **13**, 2754–2757.
32 A. R. Bogdan and K. James, *Chem.–Eur. J.*, 2010, **16**, 14506–14512.